Thermal performance investigation and optimization of a novel V-shaped finned latent heat storage unit

Kunxiao CHEN, Qiang ZHANG*

School of Energy and Power, Jiangsu University of Science and Technology, Zhenjiang, 212003, China

*Corresponding author; E-mail: zhangqJUST@163.com

The low thermal conductivity of phase change materials limits the thermal performance of heat storage devices, hindering their widespread application in engineering. To address this challenge, this paper focused on the fin design of a horizontal triplex-tube latent heat storage device. A novel V-shaped fin with a secondary arrangement is proposed. Numerical simulation is employed to investigate the effects of fin angle, fin length, and heat transfer fluid temperature on the thermal performance of the storage system. Moreover, the fin parameter is optimized by the response surface method. The results demonstrate that, compared to traditional rectangular fins, both the primary and secondary V-shaped fins can significantly enhance the thermal performance. The secondary V-shaped fin has the most significant effects, reducing the melting time of the phase change material by 48.5%, and increasing the average heat storage rate by 83.46%. Additionally, the thermal performance of the heat storage unit exhibits a trend of initially increasing and then decreasing with the increase of fin angle and length, suggesting the existence of optimal structural parameters. Consequently, the optimized secondary V-shaped fin reduces the melting time by 52.9% and increases the average heat storage rate of phase change materials by 104.48%.

Key words: *phase change material; V-shaped fin; melting characteristics; latent heat storage; response surface method*

1. Introduction

The increasing share of renewable energy, especially solar power, offers the greatest potential for CO_2 reduction and climate protection in energy industry. However, the supply of renewable energy varies greatly due to the unpredictable nature of the weather. Currently, thermal energy storage is widely recognized as a competitive solution to this challenge. It involves storing surplus thermal energy and making it available at a later time as needed. In particular, latent thermal energy storage (LTES) system with phase change materials (PCMs) has received much attention due to its high density of energy storage, stable output, and practical versatility [1]. Nevertheless, the low thermal conductivity of PCMs can observably degrade the rate of heat storage and release. In this regard, various approaches to enhance the thermal performance of PCMs, such as the incorporating nanoparticles [2] with high thermal conductivity into PCMs and the cascade utilization of multiple

PCMs [3,4], have been explored. Notably, embedding metal fins in PCMs to increase heat exchange surface area has also been proposed, mainly because of its relative simplicity and effectiveness compared to others [5].

Since fin geometry can have insignificant effects on the thermal performance, various fin shapes with different layouts for phase change enhancement of LTES system have been introduced. Safari *et al.*[6] compared the effects of straight and bifurcated fins on melting behavior of paraffin. In their study, both the fin configuration and fin parameters at different melting temperatures were considered. It is found that the bifurcated fin outperformed the straight fin for all cases considered. Ren *et al.* [7] designed a new rotating case of Y-shaped cross-fin Triplex-tube latent heat system. They found that the increase of fin length can significantly improve the thermal energy storage efficiency of TTES, However, once the fin depth L exceeds 13 mm, the heat transfer indices of TTES show only marginal improvement, particularly in thermal energy storage rate and density. In recent years, many scholars have endeavored to the development of bionic fin for LHS systems. For example, Ren *et al.*[8] proposed an irregular snowflake fin structure and optimized the fin structure. The results showed that the melting time using the snowflake fins was reduced by 45.92% compared with that of traditional fin. Wu *et al.*[9] numerically investigated the thermal energy release performance with the spiderweb-like fin for a LHS device by the enthalpy-porosity method. They found that the designed fin could effectively improve the overall solidification of PCM than the plate fin. However, the poor fin efficiency related to the proposed fin brought a larger radial temperature gradient of LTES device.

Among different popular fin shapes, V-shaped fin is one of the most visible options due to its favorable performance. The interesting features of this type of fin are the simple shape and easy processing. Moreover, Lorenzini *et al.*[10] found that the thermal resistance of V-shaped structure can be reduced by optimizing the fin shape. Alizadeh *et al.*[11] conducted a comparative study to assess the effectiveness of two enhancement methods, namely the using of V-shaped fins and the incorporation of nanoparticles, on enhancing the solidification process in a triple-tube energy storage system. The simulation results revealed that the optimized V-shaped fin was more reasonable to achieve the maximum capacity of energy storage. Lohrasbi *et al.*[12] utilized the multi-objective response surface method (RSM) to optimize the array and structural parameters of V-shaped fin for the solidification process of PCM in an LTES system. Taken energy storage capacity as optimal objective, the results indicated that the optimized longitudinal V-shaped fins could shorten the solidification process by 5.65 times compared with the absence of fins. Yao *et al.*[13] introduced a novel V-shaped fin structure for a triplex-tube LTES system. According to their study, the optimal fin design could reduce the melting time of the PCM by 31.92%under the optimal conditions. Guo *et al.*[14] suggested that the melting of PCM could be greatly accelerated by employing eccentric V-shaped fins with the reasonable arrangement. To uniform the heat transfer in the difficult-to-solidify region of PCM, Guo *et al.*[15] designed a novel two-stage V-shaped branch fin for a triple-tube LHS unit. They reported that fin length ratio primarily affected the evolution of phase interfaces.

As seen from the literature overview, attaching various bifurcated or biomimetic fins in PCMs has been proven to enhance thermal storage performance of LTES device. However, some of these fins are relatively complex which may result in the increased thermal resistance and fin volumes. Therefore, the design of simpler fin (i.e. V-shaped fin) with better thermal performance for the LTES applications is definitely meaningful. Moreover, the majority of exiting studies dealt with the design of V-shaped fins for specific LHS units. Few of them emphasized further bifurcating the V-shaped fin for

thermal performance improvement, particularly taking into account the dual-heat source in the triplex-tube latent LTES device. Accordingly, this study aims to propose a novel design of primary and secondary V-shaped fin for a triplex-tube LTES device by numerical simulation. The concept of a "dual heat source" is introduced to analyze the effects of fin structural parameters on thermal storage performance, and the optimization of fin parameters is conducted through the response surface method. The outcome of this study is expected to provide valuable guidance on fin optimization of the horizontal triplex-tube LTES unit.

2. Model establishment and numerical methods

2.1. Physical model

The novel V-shaped fins for the LTES unit are developed as shown in Fig. 1 (a). The straight fins are originally designed. Four baseline fins are attached to the surfaces of the inner and middle tubes, respectively. Thereafter, each straight fin is replaced with the V-shaped fin, namely the primary V-shaped fins. The thickness of each fin is half of the straight fin, while maintaining the same fin length and location to further increase the heat transfer area of fins, each primary V-shaped fin is further grown into two small secondary V-shaped fins. These two derived fins are distributed symmetrically on surfaces of tubes with the same circumferential position. For all cases, the fin volume remains fixed. The fin length is L, and the fin thickness is W, the fin angle is denoted as θ, with subscripts "1" and "2" representing the inner and outer sides respectively, as showed in Fig.1 (b).

In the present study, the triple-tube LTES unit is used for solar energy storage. It consists of three concentric copper tubes with diameters of 180, 150, and 42mm for the outer, middle, and inner tubes, respectively. The phase change material of paraffin RT (RT35) is encapsulated in the middle tubes. Two streams of high-temperature water flow through the inner and outer tubes, which are considered as dual heat sources to transfer heat with PCM. The thermal properties of each material are shown in Tab. 1.

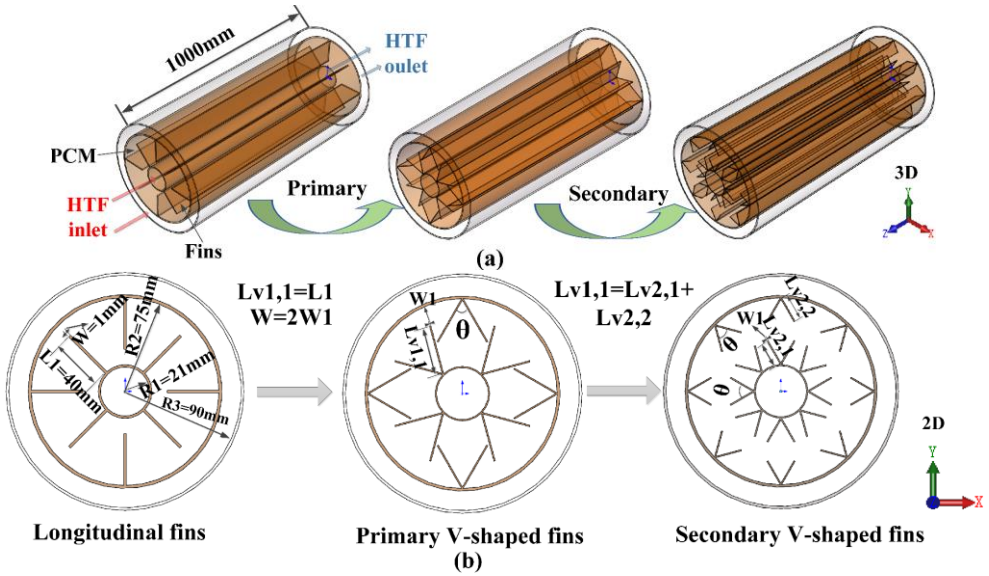

Fig. 1. V-shaped design schematic: (a) 3D model schematic; (b) 2D model schematic

Tab. 1. Physical properties of each material [16]

Physical properties	PCM (RT35)	Fin (Copper)
Density [kg·m^{-3}]	770	8978
Specific heat [J·kg^{-1}·K^{-1}]	2000	381
Thermal conductivity[W·m^{-1}·K^{-1}]	0.2	387.6
Latent heat [kJ·kg^{-1}]	170	--
Dynamic viscosity [Pa s]	0.023	--
Thermal expansion coefficient [K^{-1}]	0.0006	--
Solid phase temperature [K]	302	--
Liquid phase temperature [K]	308	--

2.2. Governing equation

In this study, the enthalpy-porosity method [8, 9, 10] was adopted for simulating the melting process of RT35. This method utilizes enthalpy and temperature as the variables to establish uniform governing equations, which can effectively reduce the cost of numerical calculation. Based on the enthalpy-porosity model, some assumptions are made as follows:

(1) The liquid PCM is laminar and incompressible flow [8];

(2) the volume change of the PCM, viscous dissipation, and heat loss at the outer surface of the tube are ignored [17];

(3) The thermal properties of PCM remain constant at the operating temperature, while its density follows the Boussinesq approximation [18];

Considering above mentioned assumptions, the governing equations for the 2-D computational domain are given as follows [18]:

Continuity equation:

$$\nabla \cdot \vec{V} = 0 \tag{1}$$

Momentum equation:

$$\rho \cdot \frac{\partial \vec{V}}{\partial t} + \rho \vec{V} \cdot \left(\nabla \cdot \vec{V}\right) = -\nabla P + \mu \nabla^2 \vec{V} + \rho \xi g\left(T - T_{ref}\right) + \vec{S} \tag{2}$$

The momentum source terms $\vec{S}$ is represented as:

$$\vec{S} = \frac{(1-\beta)^2}{(\beta^3+0.001)} A_{mush} \vec{V} \tag{3}$$

Energy equation:

$$\frac{\partial}{\partial t}(\rho H) + \nabla \cdot \left(\rho \vec{V} H\right) = \nabla \cdot (k \nabla T) - \rho L_H \frac{\partial \beta}{\partial t} \tag{4}$$

where A_{mush} is the constant for the mushy zone, it is set to 10^5 according to reference [19]. $\vec{V}$ is the velocity vector [m/s], βrepresents the liquid fraction,$\xi$is the thermal expansion coefficient of the PCM, [K^{-1}], and T_{ref} is the reference temperature, [K]. H is the total enthalpy [kJkg^{-1}], ρrepresents density, [kgm^3], t is time, [s], c, λ and ρ represent specific heat, [kJ(kgK^{-1})], thermal conductivity, [W(mK)$^{-1}$], and dynamic viscosity, [Pa s] respectively, p is pressure, [Pa], L is the latent heat of PCM, [kJkg^{-1}].

The total enthalpy H is the summation of sensible enthalpy and latent enthalpy[20]:

$$H = h_{ref} + \int_{T_{ref}}^{T} c_p \, dT + \beta L \tag{5}$$

where β is the liquid fraction of PCM, which can be expressed by:

$$\beta = \begin{cases} 0, & T < T_{solid} \\ \frac{T - T_{solid}}{T_{liquid} - T_{solid}}, & T_{solid} < T < T_{liquid} \\ 1, & T_{liquid} < T \end{cases} \quad (6)$$

where T_{solid} and T_{liquid} represent the temperature of solid and liquid PCM, respectively, [K].

2.3. Initial and boundary conditions

The initial temperature of PCM and water is set to 297.15 K and 353.15 K, respectively：

$$\begin{cases} t = 0, T_{PCM} = T_{ini} = 297.15K \\ t > 0, r = R_1, T = T_{HTF-w} = 353.15K \end{cases} \quad (7)$$

where T_{ini} represents the initial temperature, $T_{HTF\text{-}w}$ denotes the wall temperature of the conduit through which the heat transfer fluid flows.

The temperature of the outer tube wall is set to be adiabatic：

$$r = R_3, \frac{\partial T}{\partial r} = 0 \quad (8)$$

The heat transfer between the fins and the PCM is considered continuous, and the contact surface is governed by a coupled boundary condition：

$$\begin{cases} T_{fin} = T_{PCM} \\ -\lambda_{fin} \frac{\partial T_{fin}}{\partial \vec{n}} = -\lambda_{PCM} \frac{\partial T_{PCM}}{\partial \vec{n}} \end{cases} \quad (9)$$

2.4. Evaluation indicators

The performance evaluation indexes for the PCM include the total heat storage and the average heat storage rate, which are expressed as below.

The heat storage capacity is given by [19]：

$$Q_{tot} = mc_p(T - T_{ini}) + mL\beta \quad (10)$$

where Q_{tot} is the total heat storage capacity, [kJ], and m is the mass of PCM, [kg].

The average heat storage rate is expressed as[21]：

$$\Psi = \frac{Q_{tot}}{t} \quad (11)$$

where t denotes the total melting time of PCM, [s].

2.5. Model Validation

To have a robust and effective result, the independent analysis of numerical simulations is firstly performed using three total mesh numbers (11386, 23880, and 42804) and time steps (0.01s, 0.05s, and 0.1s). The verification results are shown in Fig.2. As shown in Fig. 2(a), there is a change magnitude of 0.08% and a very small relative error. Hence, the grid number of 23880 provides higher accuracy. Additionally, Fig. 2(b) shows that for time steps of 0.01s and 0.05s, the relative error with a change magnitude of 0.016% after 500s. Therefore, a grid number of 23880 and a time step of 0.05s are selected.

To validate the reliability of the simulation results, a comparison is then made between the numerical predictions from the present model and experimental data from Mat et al. [22]. As can be seen in Fig. 2(c), the maximum relative error between simulation results and test values is 2.55%. The above verification results show that the numerical model of this paper is reliable.

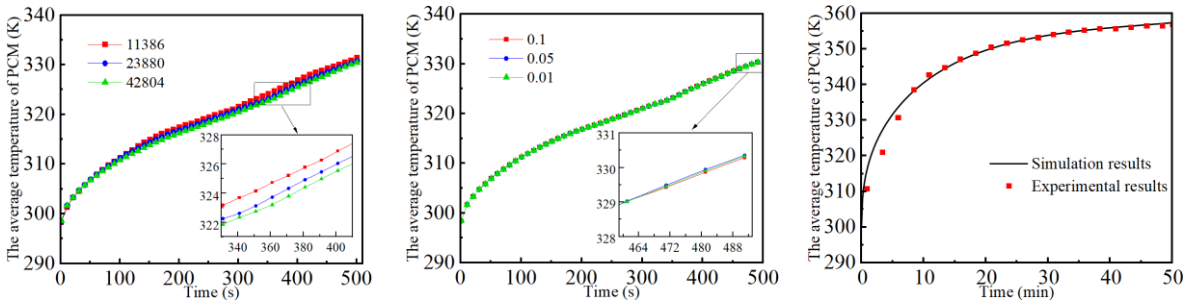

Fig. 2. (a) Verification of grid independence;(b)time step independence; and (c) Experimental validation of PCM melting by Mat *et al* [22]

3. Results and discussion

3.1. Comparative analysis of different cases

Fig. 3 shows the cloud diagram of the liquid fraction and temperature in the LTES system with different fin structures. It can be seen that at the initial duration stage (t<100s), since the fin has high thermal conductivity, the PCM contacted with the fin and tube wall starts to melt in all cases. However, the thickness of the melted film is smaller, so heat transfer undergoes with heat conduction. As the increase in amount of melted PCM, the heat transfer process is gradually dominated by natural convection. Since liquid PCM has a higher temperature and lower density, it moves upwards under the action of thermal buoyancy, leading to the accumulation of a large amount of liquid PCM in the top part of the heat storage unit. After t > 200s, irregular molten zones appear in all structures containing PCM. With the proceeding of PCM melting (i.e., 300<t<400 s), the liquid fraction and temperature distribution reveals distinct characteristics for the considered fins, with the unmelted core predominantly surrounded by the fin profile. For the secondary V-shaped fin, the PCM near the adjacent fins melts more rapidly, resulting in a very small annular solid region. Although the primary V-shaped fin can effectively partition the PCM into discrete melting regions, the liquid PCM zone is still large as shown in Fig.3. This is mainly because the natural convection is weakened in the area between the adjacent fins. As expected, the PCM with conventional rectangular fin melts locally near the heated wall boundaries, maintaining a more uniform and predictable melting profile due to the low distribution density of fins. At t=500s, it is found that the melting of PCM with the secondary V-shaped fin is almost completed, while the traditional rectangular fins shows worsen performance. Overall, the secondary V-shaped fin stands out in enhancing heat transfer compared with other two fin configurations.

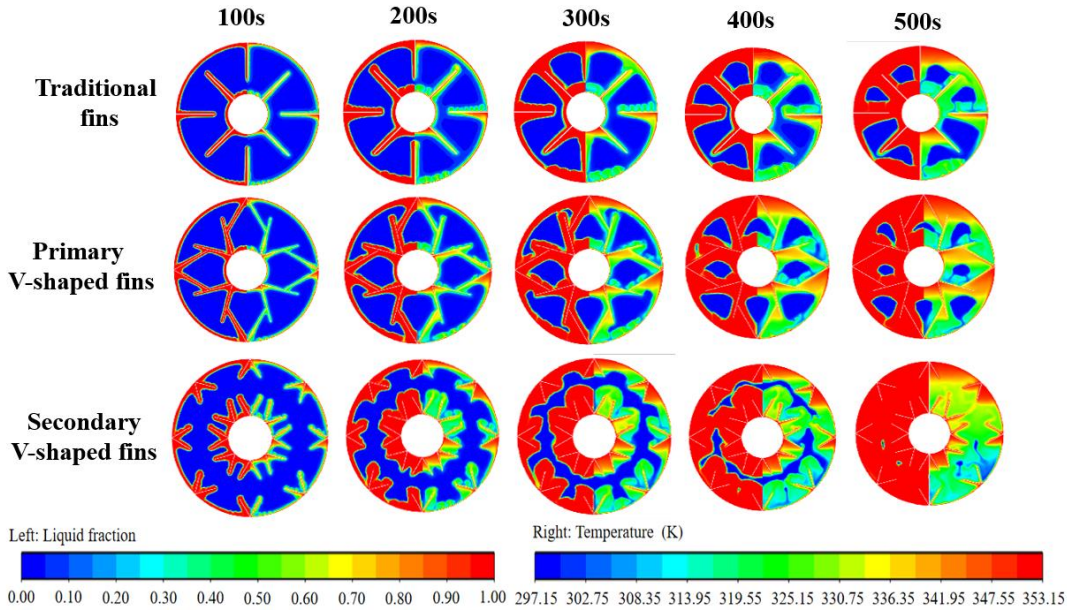

Fig. 3. The liquid fraction and temperature evolution of PCM in different cases

Fig.4 illustrates the variation of PCMvelocity (t=300s) in LTES system for different fin configurations. It can be found in Fig.4 that the velocity distribuiton of PCM varies singnificantly with variousmodificaitons of fin shape, due to the effect of natural conveciton during PCM melting. It can be found in Fig.4(a) that for the traditional rectangular fin, the votexes occur mainly in the liquid PCM layer near thesurfacesof fin and tube wall, where the the liquid PCM content increases due to the large temperature differnece between fin and PCM. Propelled by thermal buoyancy, the melted PCM movs upward and thenatural convection is enhenced gradually. Consequently, the red liquid region that representslarge flow velocity is enlarged in the upper part of the LTES unit, as shown in Fig.4(b). It is evident that the PCM in the middle part of the LHS unit is more prone to forming melting “dead zone” for the traditional rectangular fin and the primary V-shaped fin. It implyes that the long fin in these two cases may impede the development of natural convection during PCM melting. Conversely, the large velocity zonesin Fig.4(c) appears througout the LHS unit. This can be explained that the high distribution density of secondary V-shaped fin can promotesthe heat transferetowards different directons along the short fin body, andthe heat reaches the fin tipmore faster. Thus, both the natural conveciton and thermal conduciotn in the PCM are enhenced.

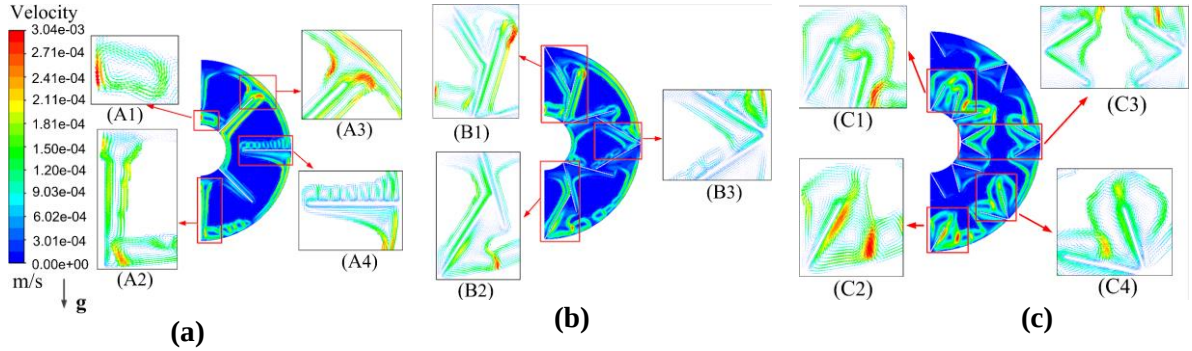

Fig. 4. The flow vector diagram of PCM with different fins: (a) traditional rectangular fins; (b) primary V-shaped fins; (c) secondary V-shaped fins

Fig.5 presents the thermal storage performance of the LTES system for three fin structures. As depicted in Figs. 5(a) and (b), compared to the traditional rectangular fin, the primary and secondary V-shaped fins reduce the PCM melting time by 30.04% and 48.5%, respectively, and the increase in the average heat storage rate is 40.37% and 83.46%, respectively. Furthermore, the average temperature of PCM with the secondary V-shaped fin structure is the highest among the three considered cases. Compared with the primary V-shaped fins, the performance of the secondary is better with a reduction in melting time by 26.39% and an increase in the average heat storage rate by 30.7%. This phenomenon arises from the enhanced natural convection due to increased heat transfer area. Fig.5(c) illustrates the similar trends in the average heat storage rate for three fin structures. In the initial melting, the average heat storage rate decreased rapidly, and then reduced gradually with the increasing melting time. Since the secondary V-shaped fin structure exhibits superior performance, the effects of structural parameters on heat storage performance using this fin structure are investigated in the following sections.

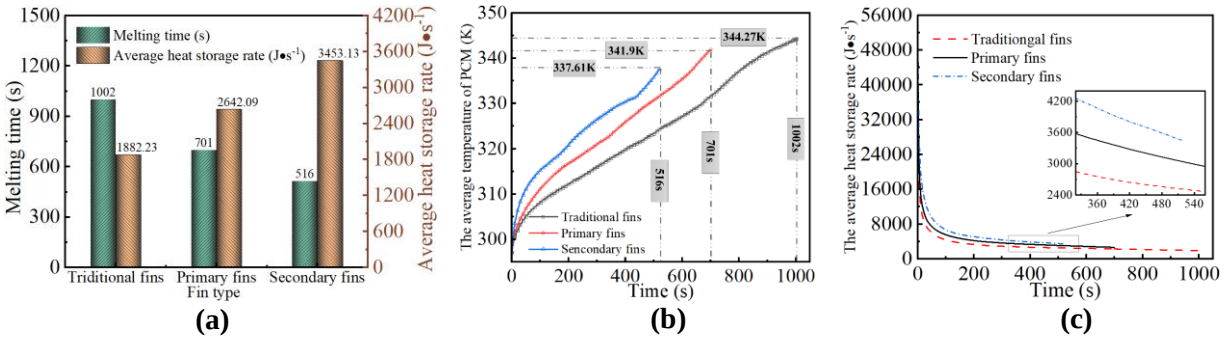

Fig. 5. Melting characteristics of PCM for different fin structures: (a) Thermal energy storage performance; (b) Average temperature of PCM; (c) Trends in the average heat storage rate

3.2. Effect of fin angle on heat transfer performance

In this study, fin angles (θ) ranging from 30° to 90° are selected as the main design parameters. Fig.6(a) reveals a decrease in PCM melting time as the fin angle increases from 30° to 60°. However, the melting time increases when the angle further increases to 90°, suggesting that an excessively large angle for the sub-V fin is not optimal. Fin angles that are too small would result in non-uniform heat transfer and may lead to the formation of a melting "dead zone". Since natural convection dominates the melting process in the middle and later stages, a large angle of the fins could weaken the natural convection process. Thus, the melting rate of PCM with the fin angle of 90° gradually slows down after 150s. Fig.6(b) indicates that a fin angle of 60° yields the shortest PCM melting time and the highest average heat storage rate. This can be attributed to the more uniform heat distribution at 60° fin angle, resulting in a larger area for the liquid-phase zone during the early duration of PCM melting, thereby facilitating the advancement of natural convection.

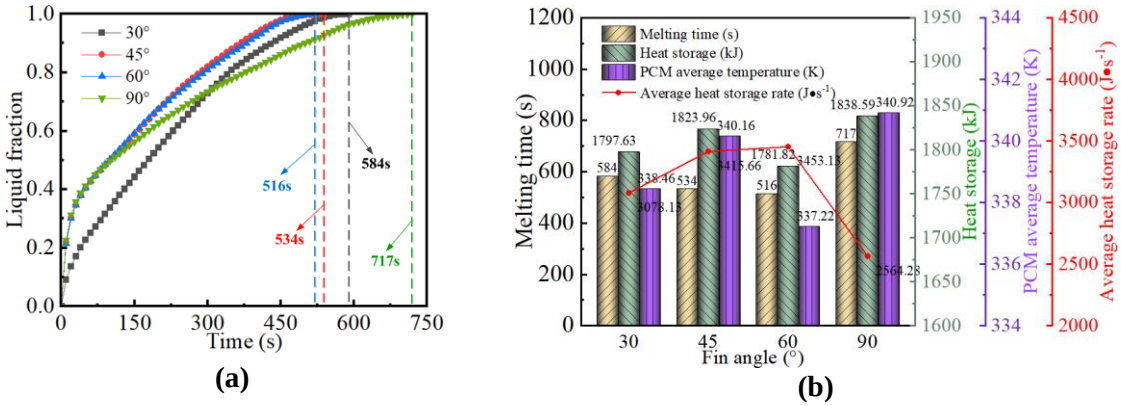

Fig. 6. Melting characteristics of PCM with different fin angles: (a) Liquid fraction; (b) Effects of different fin angles on thermal storage performance

3.3. Effect of fin length on heat transfer performance

Fig.7 shows the influences of different fin length combinations on the thermal storage performance. Five fin length combinations, which are Case 1 (10mm and 30mm), Case 2 (15mm and 25mm), Case 3 (20mm and 20mm), Case 4 (25mm and 15mm), and Case 5 (30mm, and 10mm), are considered while keeping the total fin length remains constant. As can be seen in Fig.7(a), at first there is no visible difference in melting performance for all cases. However, in the later melting process, the melting rate of Case 1 is faster than Case 5, and Case 2 outperforms Case 4. Moreover, the fin structure in Case 3 exhibits the best performance. This reveals that the combination of fin lengths for the inner and outer tubes significantly influences the melting process during the middle and late stages. The improvement in melting performance can be obtained when the fin structure is configured as "short inner and long outer". Fig.7(b) indicates that the average heat storage rate increases initially and then decreases with increasing fin length of the inner tube. Particularly, when the fin lengths of the inner and outer walls are equivalent, the average heat storage rate reaches its maximum.

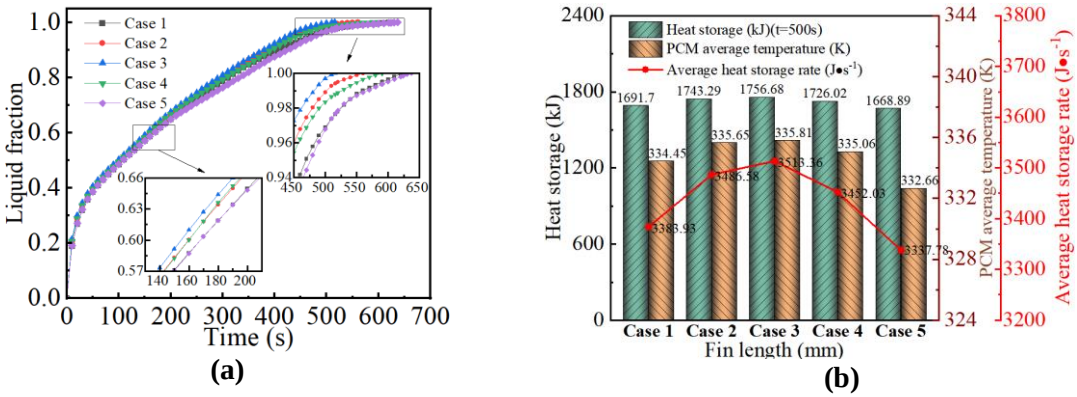

Fig. 7. Effects of different fin length combinations on the thermal storage performance: (a) Variations of liquid fraction; (b) Variations of heat storage

3.4. Effect of HTF temperature on heat transfer performance

Fig.8 shows the impact of heat transfer fluid (HTF) temperature on heat storage performance. Five different HTF temperature values (343.15 K, 348.15 K, 353.15 K, 358.15 K, and 363.15 K) are considered. It can be seen that the higher the HTF temperatures, the shorter the melting times and the higher the average temperatures of PCM. This is because the fact that the higher the HTF temperature,

the greater the temperature difference for heat transfer, resulting in a stronger driving force for heat transfer. By elevating the temperature from 343.15 K to 363.15 K, the melting time reduces by 30.08%, and the average heat storage rate increases by 38.71%.

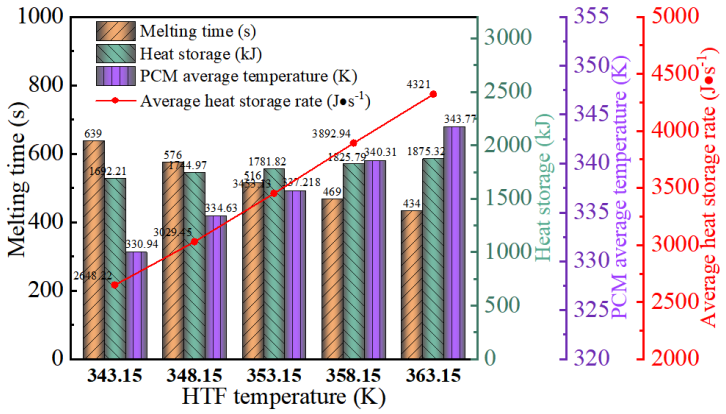

Fig. 8. Effects of different temperatures of HTF on heat storage performance

3.5. Optimization of fin structure based on RSM

In this paper, the fin parameters of the secondary V-shaped fin were optimized by using RSM, including fin thickness(0.5mm~1mm), fin length(15mm~25mm), and fin angle(35° ~65°).The total melting time of PCM is considered as the optimization objective. Box-Behnken design (BBD) was employed to conduct 17 experiments.

Tab. 2 shows the results of variance analysis for the melting time of PCM. It can be seen that F=20.41and P＜0.01, indicating that the prediction model has the statistical significance. Moreover, the F-value of the fin length (B) is the biggest (i.e., 36.30) among three factors, which means the PCM melting time is more sensitive to the change in fin length. This is because of the dominant influence of natural convection during the PCM melting, while fin length exerts main effects on this phenomenon.

Tab. 2. Results of variance analysis on PCM melting time

Source	Sum of squares	Degrees of freedom	Mean squares	F-value	P-value	Significance
Model	27261.62	9	3029.07	20.41	0.0003	significant
Fin thickness (A)	3951.60	1	3951.60	26.63	0.0013	
Fin length (B)	5387.22	1	5387.22	36.30	0.0005	
Fin angle (C)	57.24	1	57.24	0.3857	0.5542	
AB	23.52	1	23.52	0.1585	0.7024	
AC	8.12	1	8.12	0.0547	0.8217	
BC	78.32	1	78.32	0.5277	0.4911	
A^2	677.78	1	677.78	4.57	0.0699	
B^2	6682.22	1	6682.22	45.03	0.0003	
C^2	8924.01	1	8924.01	60.13	0.0001	

Considering the non-linear relationship between fin parameters and optimization objective, a regression equation for the melting time is fitting from data analysis, as shown in Eq. (12). Based on

the regression equation, the significance levels of various factors can also be obtained. It can be seen that the coefficient of fin length (L) is the largest, followed by fin thickness (W), and fin angle (θ). It means that the fin length has the most significant impact on the melting time of PCM, which is consistent of the F-value results shown in Tab.2.

$$Melting\ time=483.5-22.22W+25.95L-2.67\theta+2.42WL+1.43W\theta+4.42L\theta+12.69W^2 +39.84L^2+46.04\theta^2 (0.5\leq W\leq 1,\ 15\leq L\leq 25, 35\leq\theta\leq 65) \quad (12)$$

Fig.9 illustrates the results of response surface test with fin geometry and PMC melting time. The blue zone in Fig.9 has the smallest melting time of PCM. According to the response surface diagram, the reasonable values of fin structure for practice implement can be determined. It is evident in Figs 9(a) or (b) that when the fin angle (or fin length) is fixed, the melting time decreases with the increase in fin thickness. This trend mainly results from the reduction in PCM volume, therefore the heat storage capacity. The large value of fin thickness is suggested under this condition. Conversely, when fin length (or fin angel) increases, the melting time initially decreases, and then increases as show in Figs 9(a) and (b). This means the there is an optimal value of fin length (or fin angel) which is required to be optimized. The fin length and fin angel are expected to be in the range of 15.3-20.5 mm and 49.0-55.2°, respectively. Fig.9(c) demonstrates that the blue area is located almost at the center of the response surface diagram when the fin thickness remains constant. Accordingly, the favorable values for fin length and fin angel is narrowed to17.6-19.3 mm and 48.0-53.1°, respectively. This indicates that too large or too small values for the fin length and fin angel would lead to weak natural convection during the melting.

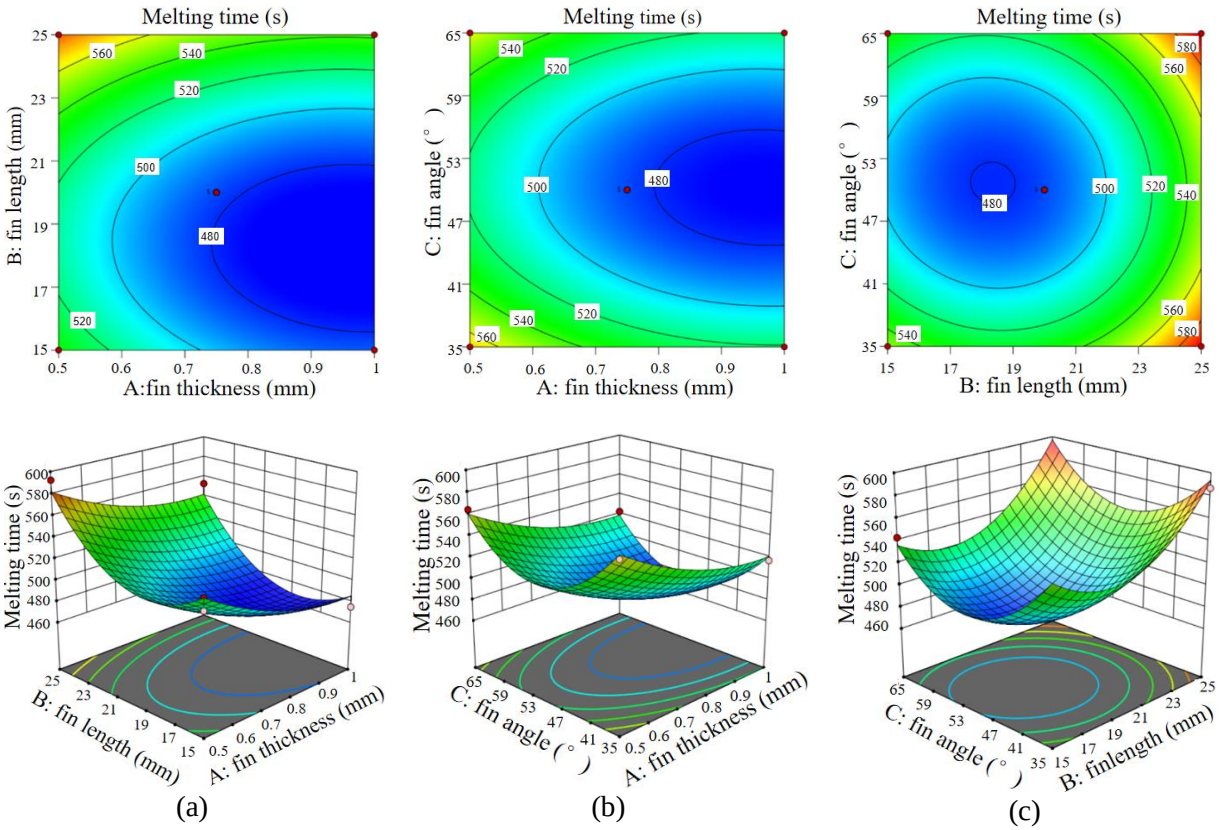

Fig. 9. The results of response surface test: (a) Fin angle is constant; (b) Fin length is constant; (c) Fin thickness is constant

According to the abovementioned analysis, the optimal design for the fin angle, fin thickness, and fin length are 52.88°, 0.9mm, and 19.1mm, respectively. At the optimal conditions, the melting time and heat storage are 471.896s and 1816.19 kJ respectively, and the average heat storage rate is 3848.71J/s. Compared with the traditional and pre-optimization fin configuration, the increase in the average heat storage rate is104.48% and 11.46%, respectively, and the melting time reduction is 52.9% and 8.5%, respectively.

4. Conclusions

In this study, the numerical investigation of melting processes in a novel V-shaped finned triplex-tube LTES system is presented. The optimal structural parameters of the proposed fin are determined by employing RSM, and compared with the traditional rectangular fins to demonstrate its effectiveness. The main conclusions are as follows:

(1) Compared to the traditional rectangular fins, the primary and secondary V-shaped fin reduces the melting time by 30.04% and 48.5% respectively, and boosts the average heat storage rate by 40.37% and 83.46% respectively.

(2) The fin angle and fin length play crucial roles in determining the heat storage performance of the heat storage unit. Excessively long fins would impede the natural convection process, while unsuitable fin angles may disrupt the uniformity of heat transfer. Making a good trade-off between these parameters is essential for maximizing the heat storage efficiency.

(3) Under optimal conditions, the secondary V-shaped fins could reduce the PCM melting time by 52.9% and increase the average heat storage rate by 104.48% compared to traditional rectangular fins. Moreover, the melting time is reduced by 11.46% compared to the secondary V-shaped fins without optimization.

The outcomes of this study can provide valuable guidance on design of the horizontal triplex-tube LTES system. Further research (i.e., the multi-objectives optimization of fin geometry, and small-scale experimental study, etc.) is still required for enhancing the performance of the proposed system.

Nomenclature

Cp	- specific heat [$J\cdot(kg\cdot K)^{-1}$]	β	-liquid fraction
G	- gravity coefficient [$m\cdot s^{-2}$]	θ	-fin thickness [mm]
ΔH	- latent heat enthalpy [J]	ξ	-the thermal expansion coefficient [K^{-1}]
L	- latent heat[$J\cdot kg^{-1}$]		
m	-mass[kg]	μ	-dynamic viscosity [Pas]
p	-pressure [Pa]	ψ	-average heat storage rate [$J\cdot s^{-1}$]
Q	-heat storage [kJ]	*Acronyms*	
S	-source term	*BBD*	-Box-Behnken design
t	-time [s]	*HTF*	-heat transfer fluid
T	-temperature [K]	*LTES*	-latent thermal energy storage
W	-fin thickness [mm]	*LHS*	-latent heat storage
Greek symbols		*PCM*	-phase change material
λ	-thermal conductivity [$W\cdot(m\cdot K)^{-1}$]	*RSM*	-response surface method

References

[1] Low, Z.H., *et al.*, A review of fin application for latent heat thermal energy storage enhancement, *Journal of Energy Storage, 85* (2024), 111157.

[2] Ranjbar, A.A., *et al.*, Numerical heat transfer studies of a latent heat storage system containing nano-enhanced phase change material, *Thermal Science, 15* (2011), 1, pp. 169-181.

[3] Nagappan, B., *et al.*, Heat transfer enhancement of a cascaded thermal energy storage system with various encapsulation arrangements, *Thermal Science*, *23* (2019), 2, pp. 823-833.

[4] Zhang, Q., *ea al*, Investigation on thermo-economic performance of shipboard waste heat recovery system integrated with cascade latent thermal energy storage, *Journal of Energy Storage, 64* (2023), 107171.

[5] Khedher, N. B., *et al.*, On the application of novel arc-shaped fins in a shell-and-tube type of latent heat storage for energy charge enhancement, *Journal of Energy Storage*, *73* (2023), 108697.

[6] Safari, V., *et al.*, Experimental and numerical investigations of thermal performance enhancement in a latent heat storage heat exchanger using bifurcated and straight fins, *Renewable Energy*, *174* (2021), pp. 102-121.

[7] Ren, F., *et al*, Investigation and optimization on a Y-shaped fins for phase change heat storage by rotational mechanism, *Journal of Energy Storage*, 94 (2024), 112436.

[8] Ren, F., *et al.*, Optimization on a novel irregular snowflake fin for thermal energy storage using response surface method, *International Journal of Heat and Mass Transfer*, *200* (2023), 123521.

[9] Wu, L., *et al*, Numerical analysis and improvement of the thermal performance in a latent heat thermal energy storage device with spiderweb-like fins. *Journal of Energy Storage*, 32 (2020), 101768.

[10] Lorenzini, G., *et al.*, Constructal design of Y-shaped assembly of fins, *International Journal of Heat and Mass Transfer, 49* (2006), 23-24, pp. 4552-4557.

[11] Alizadeh, M., *et al.*, Solidification acceleration in a triplex-tube latent heat thermal energy storage system using V-shaped fin and nano-enhanced phase change material, *Applied Thermal Engineering*, *163* (2019), 114436.

[12] Lohrasbi, S., *et al.*, Response surface method optimization of V-shaped fin assisted latent heat thermal energy storage system during discharging process, *Alexandria Engineering Journal*, *55* (2016), 3, pp. 2065-2076.

[13] Yao, S., *et al.*, Evaluation and Optimization of the Thermal Storage Performance of a Triplex-Tube Thermal Energy Storage System with V-Shaped Fins, *Journal of Thermal Science, 32* (2023), 6, pp. 2048-2064.

[14] Guo, X. H., *et al.*, Effect of eccentricity and V-shaped fins on the heat transfer performance of a phase change heat storage system, *Journal of Energy Storage*, *73* (2023), 108833.

[15] Guo, H., *et al.*, Enhancing the energy discharging performance by novel V-shaped branch fins in a triple-tube latent heat storage unit, *Journal of Energy Storage*, *73* (2023), 108833.

[16] Kousha, N., *et al.*, Experimental investigation of phase change in a multitube heat exchanger, *Journal of Energy Storage*, *23* (2019), pp. 292-304.

[17] Pu, L., *et al.*, Numerical study on the performance of shell-and-tube thermal energy storage using multiple PCMs and gradient copper foam, *Renewable Energy*, *174* (2021), pp. 573-589.

[18] Zhang, C. B., *et al.*, Improving the energy discharging performance of a latent heat storage (LHS) unit using fractal-tree-shaped fins, *Applied Energy*, *259* (2020), 114102.

[19] Abreha, B. G., *et al.*, Thermal performance evaluation of multi-tube cylindrical LHS system, *Applied Thermal Engineering*, *179* (2020), 115743.

[20] Huang, Y., *et al.*, Experimental and numerical studies on the heat transfer improvement of a latent heat storage unit using gradient tree-shaped fins, *International Journal of Heat and Mass Transfer*, *182* (2022), 121920.

[21] Yu, C., *et al.*, Melting performance enhancement of a latent heat storage unit using gradient fins, *International Journal of Heat and Mass Transfer*, *150* (2020), 119330.

[22] Mat, S., *et al.*, Enhance heat transfer for PCM melting in triplex tube with internal-external fins, *Energy Conversion and Management*, *74* (2013), pp. 223-236.

Received: 18.06.2024.

Revised: 22.07.2024.

Accepted: 25.07.2024.